Response to Takashi Obase (RC2)

We want to thank the reviewer for their effort and the very helpful comments on our manuscript. Below find detailed answers to all comments. The reviewer's comments are in blue, our answers in black and in *italic* we show specific modifications to the original manuscript.

General comments

[1] As in the abstract and conclusion, one primary finding is that the hysteresis of the Greenland ice sheet is identified near glacial conditions corresponding to -10K to -9K in regional summer temperature. However, the text does not appear to have adequately considered the assumptions that underlie the derivation of this temperature values. The equation (6) ΔTocn = 0.25ΔTann is one example. As stated in the main text, this equation uses the same equation as Golledge (2015). However, as the study of Golledge et al. (2015) is for Antarctic ice sheet, it needs some justification arguments why they identified this value. For example, In a more recent study, Garbe et al. (2020) used ΔTocn = 0.39Δ Tann for the Antarctic ice sheet, based on an analysis of the Antarctic region in a 4xCO2 climate model simulation.

I agree with using formulation (6) for all experiments in this paper, but as analyzed in additional experiments (Appendix Figure C1) and L344-348, I believe it is important to note that showing temperature values of -10 to -9 K in the conclusions and abstract contains significant uncertainty in relating atmospheric temperature to ocean temperature.

[2] I couldn't fully understand how ocean temperature works in the experiments. According to Section 2.3, if I put the parameters κ=15 and Bref=50 into Equation 5, ΔTocn=-3.33K induces Bgl=0. And using equation (6), Bgl=0 when ΔTjja=-8.89K, and below that temperature anomaly, Bgl=0 as Bgl cannot be negative (L134). However, according to Figures 6 and 7, basal mass balance is still significantly greater than 0 even if ΔTjja is around -10K.

According to my calculation above, in Figure 8, both ΔTjja=-9.3K and -9.4K would induce Bgl=0, I'm confused. Maybe I'm doing something wrong. I have a suggestion. Since Bgl should have a uniform value, I think it would be possible to plot the Bgl values on top of Figure 3. Wouldn't it make it clearer how the basal melting works?

We answer these two first comments together since they are closely related. First, we want to acknowledge that the calculations performed in comment [2] are correct. Thanks to this, we have realized that there was an error in the manuscript regarding the scaling factor value between oceanic and atmospheric temperature anomalies that remained from an earlier draft.

The actual value used is 0.22, so that with $\Delta T_{ann} = 1.5\Delta T_{jja}$ we have: $\Delta T_{ocn} = 0.22\Delta T_{ann} = 0.33\Delta T_{jja}$. In this way, for κ=15 $myr^{-1}K^{-1}$ and B_{ref}=50myr^{-1}, $B_{gl} = 0$ when $\Delta T_{ocn} = -3.33K$ and $\Delta T_{jja} = -10.1K$. That is why at around -10K of summer regional temperature anomaly, the basal melting is higher than 0. We thank the reviewer very much for bringing this mistake to our attention.

We will explicitly add this basal melting activation temperature (ΔT_{jja} = -10.1 K; ΔT_{ocn} = -3.3 K) to the revised version of the text. However, we do not consider it necessary to include B_{gl} in Fig. 3 of the manuscript, as Fig. 6 already shows the mass flux information, including total basal melting, and reflects the timing of its activation.

Regarding comment [1], the scaling factor between oceanic and annual atmospheric temperature ($f = \frac{\Delta T_{ocn}}{\Delta T_{atm,annual}}$) is indeed highly uncertain. Garbe et al. (2020) used f = 0.39 based on the value obtained for a four-fold increase in CO2 in Antarctica once equilibrium was reached with the ECHAM5–MPIOM coupled model. Golledge et al. (2015) used f = 0.25 based on the CMIP5 multi-model ensemble mean in Antarctica. However, both studies are based on inferences from the Antarctic domain and for temperatures above present-day values.

We calculated the mean ratio between oceanic and atmospheric temperature over the ocean surrounding Greenland using PMIP3 models outputs (CCSM4, CNRM-CM5, FGOALS-g2, IPSL-CM5A-LR, MIROC-ESM, MPI-ESM-P, MRI-CGCM3). This yields $f_{LGM} = 0.18 \pm 0.02$ for the LGM and $f_{Hol} = 0.5 \pm 0.2$ for the mid-Holocene. These values show considerable spread. We chose *f = 0.22* as it falls within this range and it is closer to LGM values, which is appropriate since ocean forcing has greater influence in the temperature range we investigate. We will discuss this in the main text.

Importantly, exploring the effect of κ in Eq. (5) for basal melting is equivalent to exploring the uncertainty in *f*, since this equation can also be written as: $B_{gl} = \kappa f\ \Delta T_{ann} + B_{Ref}$. As shown in Appendix C, this has a direct impact on the bifurcation point value. Higher values of *f* (like higher values of κ) shift the bifurcation point toward higher temperatures (note for the first bifurcation point $\Delta T_{jja} < 0$, therefore for higher κ Bgl = 0 is reached for lower-amplitude anomalies in absolute value). This value is therefore highly sensitive to the experimental setup (as the reviewer is pointing out), which underscores the importance of the uncertainty analysis presented in Appendix C and is the reason why we agree with the reviewer's suggestion. We will accordingly expand our discussion on this effect by acknowledging the associated uncertainty of the ocean-to-atmosphere fraction, f.

Finally, given the large uncertainties in the basal melting, we agree that there are substantial uncertainties also associated with the value of the first bifurcation point. This is what we aimed to show in Fig. C1. We agree with the reviewer's suggestion to put less emphasis on the exact value of the bifurcation point. We will therefore clarify this in the main text, abstract, and conclusions.

[3] Tabone et al (2018) is one important previous study of this article of this study because the discussion of the evolution of Greenland ice sheet is discussed (final sentence of the abstract). I find there are many improvements and changes in the model setup compared to Tabone et al. (2018). However, the manuscript does not clarify that basal freezing was possible in Tabone et al. (2018), contrary to this study. I like the setup of this study preventing basal freezing, because Antarctic Ocean modeling indicates still active basal melting in the glacial conditions because thermal forcing is

positive (Kusahara et al. 2015; Obase et al. 2017). Would it be possible that the presence or absence of basal freezing can have a substantial impact on the hysteresis?

Yes, the fact that refreezing was allowed in Tabone et al. (2018) is indeed a difference from the present study, and we will make this explicit in the text. Eliminating refreezing (by limiting basal mass balance to zero when temperature anomalies would lead to negative values) was an improvement introduced in subsequent papers (Tabone et al., 2019a; Tabone et al., 2019b; Tabone et al., 2024). While local variations in basal melting and refreezing can exist at the ice-shelf base, given our simplification of applying spatially homogeneous melting, it makes more sense to fully eliminate refreezing in the entire domain rather than allow an unrealistic amount of it. This is particularly true in light of the references cited by the reviewer (Kusahara et al., 2015; Obase et al., 2017).

Regarding whether refreezing would affect the hysteresis, evidence from previous papers (Álvarez-Solas et al., 2017; see the reviewing discussion) suggests that allowing for refreezing could enable faster regrowth in a transient run in response to sufficiently low temperatures. However, concerning the equilibrium stability diagram, refreezing would only be activated in the range of summer regional temperature anomalies of approximately -12 to -10 K, when the cooling branch recovers the LGM-like state, thus not substantially affecting the hysteresis or the main conclusions of our study.

[4] In the experiment, the atmospheric surface mass balance and the ocean basal mass balance change simultaneously in response to ΔTjja. However, an additional experiment in which one of the forcings is turned off, would identify the mechanism. For example, in the -9.3K experiment (Figure 8), if the tipping point does not occur when only Bgl is set to - 9.4K, we can strongly argue that the mechanism of MISI is oceanic forcing.

We want to thank the reviewer for this suggestion. As shown in Figure 6 of the manuscript, at this first bifurcation point only basal melting was increasing significantly (since surface mass balance remains nearly constant), making it straightforward to attribute the triggering of the MISI to oceanic processes. Nevertheless, we agree that the additional experiments suggested by the reviewer would provide final confirmation of the respective roles of atmospheric and oceanic forcing in triggering the different feedbacks along the stability diagram. Therefore, we have simulated two quasi-equilibrium experiments with a forcing rate of $3\cdot10^{-5}$ $K\cdot yr^{-1}$ under the following conditions:

- Only OCN: ΔT_{jja} remains constant (at -12 K during the warming branch and +4 K during the cooling branch, corresponding to initial state values).
- Only ATM: ΔT_{ocn} remains constant (at -4 K during the warming branch and +1.3 K during the cooling branch, corresponding to initial state values).

The initial state of both experiments is the same as in the original stability diagram (Fig. 1 in the manuscript).

We selected the same forcing rate as in on our sensitivity analysis of basal melting parameters, as it allows us to maintain simulations close to equilibrium while reducing computational costs compared to slower forcing rates (these experiments require 533 kyr versus 1.6 Myr for the quasi-equilibrium simulation with a forcing rate of $1{\cdot}10^{-5}$ K yr^{-1}). The results are presented in the Fig. R2.1, which shows both branches of the stability diagram for the OCN-only and ATM-only experiments, as well as the default quasi-equilibrium simulation with both atmospheric and oceanic forcings active.

Regarding the warming branch, the OCN-only simulation follows the control run almost exactly until ΔT_{ocn} = -1K, when the margin retreats to the coastline and reaches a constant state regardless of the increase in ocean temperature. There is no second tipping point in this simulation, which implies the latter was due to the atmospheric feedbacks. Reciprocally, the ATM-only simulation exhibits minimal changes until ΔT_{jja} = -3K (ΔT_{ocn} = -1K). At around ΔT_{jja} = -1K the ice sheet loses the northeast sector, then retreats to the present-day margin and subsequently reaches a virtually ice-free state.

Regarding the cooling branch, as expected, in the OCN-only experiment the ice sheet remains in its virtually ice-free state, given that although oceanic temperatures decrease, it is impossible for the ice sheet to grow without a decrease in atmospheric temperatures. In contrast, the ATM-only experiment follows the control run almost exactly until ΔT_{jja} = -7K, when in the control run the ice sheet recovers the marine sectors and in the ATM-only experiment the warm ocean doesn't allow the grounding line to advance.

These results confirm the findings indicated in Figure 6 of the manuscript, that ocean warming is triggering the MISI in the northeast, while atmospheric warming triggers the elevation and albedo feedbacks. In the absence of ocean forcing, there is also an abrupt loss in the northeast region, but much higher atmospheric temperatures are needed to initiate the margin retreat.

We will add the description of these experiments to Section 2.4 and the figure R2.1 with its description to Section 3.2. This will further strengthen our conclusions that oceanic warming is responsible for the first bifurcation point, while atmospheric warming triggers the feedbacks responsible for the second bifurcation point.

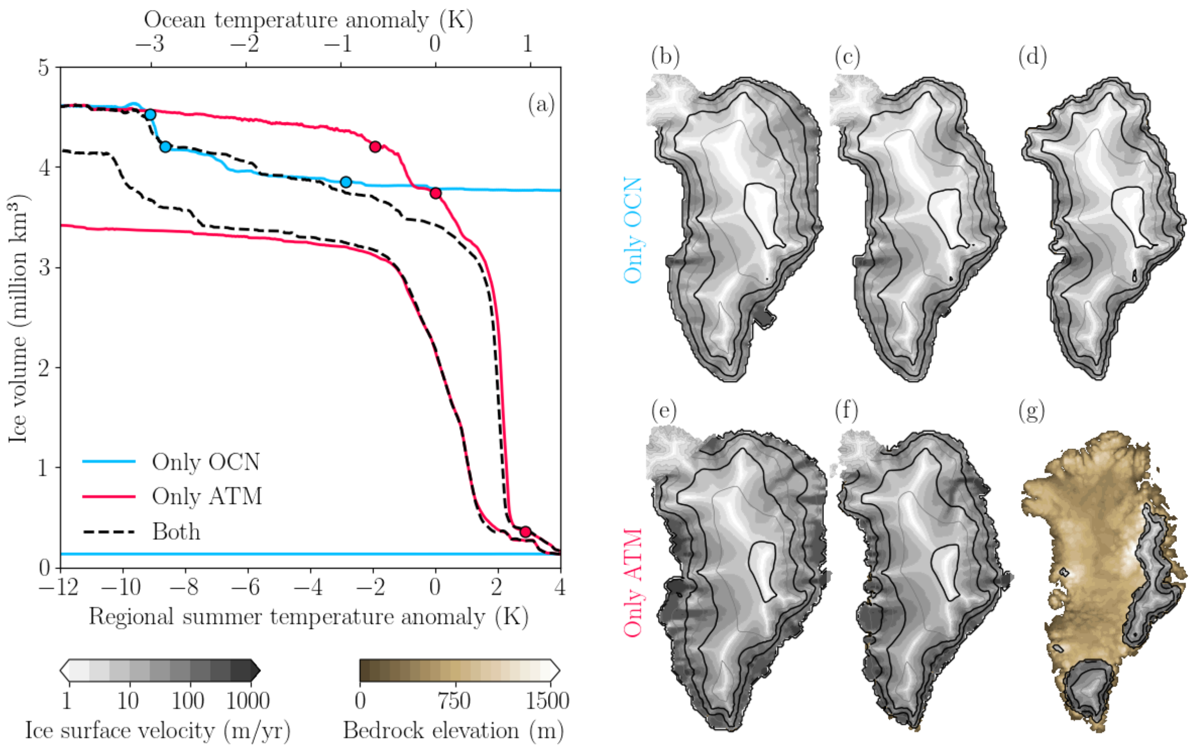

Figure R2.1: a) Ice volume above flotation for three quasi-equilibrium simulations with a forcing rate of 3×10^{-5} K yr^{-1}: (1) OCN-only simulation, maintaining regional summer temperature anomaly constant at -12 K (corresponding to the LGM-like state) during the warming branch and at +4 K (corresponding to the virtually ice-free state) during the cooling branch; (2) ATM-only simulation, maintaining ocean temperature anomaly constant at -4 K (corresponding to the LGM-like state) during the warming branch and at +1.3 K (corresponding to the virtually ice-free state) during the cooling branch; and (3) simulation with both atmospheric and oceanic forcing, same simulation presented in Fig. 3 of the manuscript. b)-d) The three snapshots of the OCN-only simulation marked with blue dots in a). e)-g) The three snapshots of the ATM-only simulation marked with red dots in a). The black contour lines in b)-g) indicate the surface elevation every 500 m starting from 0 and with a thicker line every 1000 m.

Detailed comments

L4: "global warming to 4K" would be changed to "threshold of ice-free state"?

Thanks for the suggestion, but we prefer to keep the original sentence, as we are referring to the forcing itself rather than the consequences of the forcing, which we believe is more accurate in this context.

L7-8: Please clarify that -12 K and +4K indicate regional summer temperature.

Fixed.

L34-35: On the threshold of Greenland ice sheet, recent study (Gregory et al., 2020) addresses this topic, with the effect of ice sheet-climate interactions and the irreversibility of the Greenland ice sheet.

Thanks for the suggestion, we will add that reference to the introduction.

L41: “regional summer atmospheric temperature” Where? Is it based on ice core site NGRIP?

Yes, in central Greenland. There was an error in the reference. The data is from the merged product of Buizert et al. (2018), and we will clarify this in the manuscript.

L80: Is the extent of the ice shelf margin determined only by stress alone? Are there any geographical constraints like continental shelf break positions?

The extent of ice shelves is determined by ice dynamics and mass balance (surface mass balance, basal melting, and calving). However, since the presence of ice is considered implausible in the deep ocean, calving is applied where the bedrock depth exceeds 1000m. We will make it clear in the manuscript.

L83-84: As far as I understand, the REMBO needs specific humidity as the input. According to the model results' description, an increase in regional atmospheric air temperature leads to an increase in precipitation over Greenland (e.g., L266). How is the specific humidity treated in temperature changes? Is it assuming the relative humidity as the constant?

As developed in the answer to the first reviewer, the specific humidity Q at the boundary is given by:

$$Q = Q_{sat}(T) \cdot r \, ;$$

where $Q_{sat}(T)$ is the saturation specific humidity, which depends on temperature following the Clausius-Clapeyron equation. Therefore, across the diagram, the temperature at the boundaries changes and the relative humidity is constant, but the specific humidity changes according to the temperature variations. In REMBO, the choice to maintain constant relative humidity rather than specific humidity is based on the fact that specific humidity has a stronger temperature dependence (Robinson et al., 2010).

We will clarify this in the manuscript.

L89: “100 km” which model’s resolution? I suppose the resolution of ERA-40 is ~100 km; could you please clarify this?

REMBO resolution is 100km, we will clarify this in the manuscript.

L90: According to Robinson et al. (2010), the REMBO utilized empirical lapse rate feedback of 6.5 K/km for elevation correction. Is the same elevation-temperature feedback utilized in the current model used in these experiments?

Yes, it is the same value as in Robinson et al. (2010). We will clarify this in the manuscript.

L107: Is δP defined at every 16 km grid cell? It would be helpful to put the map of P and Pcorr in the supplemental Figure

No, δP is calculated in the REMBO model, which has a resolution of 100km; therefore, δP is calculated at every 100km grid cell, and it is smoothed. Thanks for the suggestion, we will clarify this in the manuscript and we will add the figure suggested to an appendix.

L109: What does “consistent field” mean?

We mean a field consistent with the boundary conditions at each moment (topography, ΔTjja and specific humidity). Since the δP field can introduce a bias from present-day conditions, if it had no limits, it could introduce variations that would go beyond those related to the model's own bias. We will clarify this in the manuscript.

L128: Is The unit m/yr defined as "freshwater equivalent" mass balance? Or ice equivalent? Please clarify.
It is ice equivalent, we will clarify it in the manuscript.

L156: I think retaining insolation as present-day is one probable experimental design because summer insolation in the northern high latitude at the LGM is similar to present-day. However, I recommend the author consider adding one sensitivity experiment setting reduced sea level and setting LGM insolation values (used in the energy balance model REMBO as in equation 3) to assess the impact of these parameters.
This suggestion was also made by Reviewer 1. Therefore, we conducted sensitivity experiments examining the effects of varying insolation and sea-level conditions in the LGM-like initial state. As detailed in our response to Reviewer 1 (general comment #1), results show that under the insolation and sea level of the LGM some floating ice became grounded, but the overall ice-sheet configuration remains largely similar, particularly in the northeastern region. With LGM conditions (insolation and sea level), the first bifurcation point occurs at slightly higher temperatures, but still within the ocean forcing uncertainty range, and the overall system behavior is preserved.

L299: Please clarify at what degree of ΔTjja does basal melting activate?
Clarified above.

L349-L354: In Bochow's (2023) experiment, oscillations were not observed in YELMO-REMBO. However, oscillations were observed in the experiment described in this article. I have identified that the experimental design is not identical with Bochow et al. (2023), the one is the scaling ratio of ΔTjja and ΔTdjf (1.61 in Bochow et al. (2023) while the scaling ratio is 2 in this study. Are there other differences in how ocean melt is determined? I believe it would be beyond scope of this study to explain why oscillatory solutions appear in the experiments in the current setup. I recommend summarizing the differences in the experimental setup compared to Bochow et al. (2023) and stating that the existence of oscillatory solutions depends on the experimental setup.

Exactly, some of the differences with the experimental setup in Bochow et al. (2023) are: (1) the scaling ratio between summer and winter; (2) the melt parameters in the ocean melting equation (κ and B_{ref}) and the scaling factor between ocean and atmosphere; and (3) the use of a bias correction in precipitation. However, the main difference lies in the experimental design itself.

In our experiments, oscillations occur under constant forcing conditions after a transient warming or cooling phase (Fig. B1 in the manuscript). Specifically, oscillations appear at +1.4 and +1.6 K, starting at approximately 200 kyr in the warming branch and 50 kyr in the cooling branch. In contrast, Bochow et al. (2023) applied a very rapid (nearly instantaneous) warming followed by rapid cooling to different convergence temperatures, which were then held constant for 100 kyr. They did not explore what would occur if the equilibrium simulations were extended for longer periods (and at that exact temperature anomalies) and they didn't perform the cooling or regrowth branches. With longer timescales, the bedrock has more time to rebound isostatically, uplifting the surface to higher altitudes with lower temperatures. This favors ice regrowth and is the mechanism that, coupled with other feedbacks, we believe is responsible for the emergence of oscillations in our setup. However, since oscillations start on timescales longer than those explored by Bochow et al. (2023), direct comparison is not possible, as it is unclear whether extended simulations under their setup would exhibit similar behavior.

L373-L380: Please clarify that Honing (2023) defines temperature as the global mean temperature, which differs from this study and Robinson (2012).
Fixed.

L381-L386: Bochow et al. (2023) derives the relationship between global mean temperature and ΔTjja based on an analysis of the CMIP6 climate model historical and the SSP585 experiment. I recommend summarizing the method of relating global mean temperature and ΔTjja in the manuscript text.
We agree and we will clarify this methodology in the manuscript text. Following Bochow et al. (2023), we use the equation:

$$\Delta \mathrm{GMT}_{\mathrm{PI}} = f \times \Delta T_{\mathrm{JJA}} + 0.5\,^{\circ}\mathrm{C}$$

where f = 1/1.19 K^{-1}. This scaling factor represents the mean value derived from the CMIP6 SSP5-8.5 experiments (Extended Data Table 1 of Bochow et al., 2023). We use the factor derived from SSP5-8.5 rather than the one from historical simulations because in this case (L381-L386, talking about the second bifurcation point) our target regional temperature anomalies are above present-day values, making the SSP5-8.5 relationship more appropriate for future warming scenarios. Note that we use this scaling factor only when talking about the value of the second bifurcation point, this conversion wouldn't be appropriate for the first one.

L373-L380
Figure C1: It would be good to have a diagram with Mgl on the horizontal axis, which would allow us to consider whether the basal mass balance of the ocean or the surface mass balance of the atmosphere primarily determines hysteresis.
Given the new experiments performed (ATM-only and OCN-only) shown in Figure R2.1, which clearly demonstrate the effects of the ocean and atmosphere on stability, we believe it is not necessary to add the surface mass balance to this figure. Moreover, the purpose of this figure is to show the uncertainty in the first bifurcation point related to the basal melting scheme.

Other minors:
L5: Yelmo coupled with regional energy balance model REMBO
It is mentioned in the next sentence, L10.

L47: “regional climate model REMBO” to “regional energy balance model REMBO” to make consistency.
Fixed.

L82: “regional climate model” to “regional energy balance model”
Fixed.

Figure A1: Could you please show the distribution of SMB in the current climate in this experimental setting, with a comparison to SMBMIP (Fettweis et al. 2020)?
Yes, we think this is a great suggestion. However, while we simulate the present-day with the average conditions for the period 1958–2001, the ensemble from Fettweis et al. (2020) starts in 1980. This is why we also include outputs from MAR v3.14.3 at 10 km resolution, forced at its lateral boundaries by ERA5 and provided by Dr. Fettweis, which cover the period 1958–2001 and represent more recent simulations. Therefore, we believe it is more appropriate to include the latter in the revised version of the manuscript. We include the comparison below (Figure R2.2).

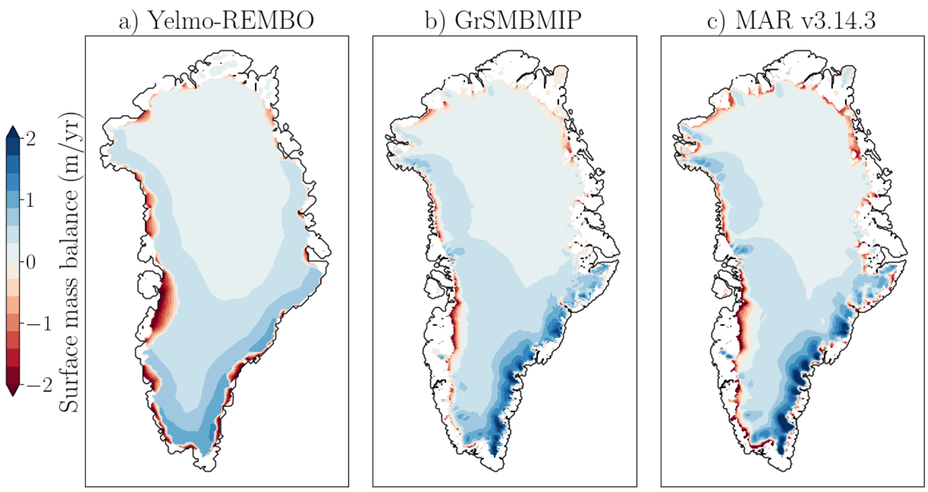

Figure R2.2: a) Yelmo-REMBO surface mass balance; b) GrSMBMIP ensemble mean for the period 1980-2001 (Frettweis et al. 2020); and c) MAR version 3.14.3 forced with ERA5, mean for the period 1958-2001. Values are expressed in meters of water equivalent per year.

References:

Alvarez-Solas, J., Banderas, R., Robinson, A., & Montoya, M. (2017). Oceanic forcing of the Eurasian Ice Sheet on millennial time scales during the Last Glacial Period. *Climate of the Past Discussions*, *2017*, 1-19.

Albrecht, T., Winkelmann, R., & Levermann, A. (2020). Glacial-cycle simulations of the Antarctic Ice Sheet with the Parallel Ice Sheet Model (PISM)–Part 1: Boundary conditions and climatic forcing. *The Cryosphere*, *14*(2), 599-632.

Buizert, C., Keisling, B. A., Box, J. E., He, F., Carlson, A. E., Sinclair, G., & DeConto, R. M. (2018). Greenland-wide seasonal temperatures during the last deglaciation. *Geophysical Research Letters*, *45*(4), 1905-1914.

Fettweis, X., Hofer, S., Krebs-Kanzow, U., Amory, C., Aoki, T., Berends, C. J., ... & Zolles, T. (2020). GrSMBMIP: intercomparison of the modelled 1980–2012 surface mass balance over the Greenland Ice Sheet. *The Cryosphere*, *14*(11), 3935-3958.

Golledge, N. R., Kowalewski, D. E., Naish, T. R., Levy, R. H., Fogwill, C. J., & Gasson, E. G. (2015). The multi-millennial Antarctic commitment to future sea-level rise. *Nature*, *526*(7573), 421-425.

Gregory, J. M., George, S. E., & Smith, R. S. (2020). Large and irreversible future decline of the Greenland ice sheet. *The Cryosphere*, *14*(12), 4299-4322.

Kusahara, K., Sato, T., Oka, A., Obase, T., Greve, R., Abe-Ouchi, A., & Hasumi, H. (2015). Modelling the Antarctic marine cryosphere at the Last Glacial Maximum. *Annals of Glaciology*, *56*(69), 425-435.

Obase, T., Abe-Ouchi, A., Kusahara, K., Hasumi, H., & Ohgaito, R. (2017). Responses of basal melting of Antarctic ice shelves to the climatic forcing of the Last Glacial Maximum and CO 2 doubling. *Journal of Climate*, *30*(10), 3473-3497.

Robinson, A., Calov, R., & Ganopolski, A. (2012). Multistability and critical thresholds of the Greenland ice sheet. *Nature Climate Change*, *2*(6), 429-432.

Robinson, A., Calov, R., & Ganopolski, A. (2010). An efficient regional energy-moisture balance model for simulation of the Greenland Ice Sheet response to climate change. *The Cryosphere*, *4*(2), 129-144.

Tabone, I., Robinson, A., Alvarez-Solas, J., & Montoya, M. (2019a). Impact of millennial-scale oceanic variability on the Greenland ice-sheet evolution throughout the last glacial period. *Climate of the Past*, *15*(2), 593-609.

Tabone, I., Robinson, A., Alvarez-Solas, J., & Montoya, M. (2019b). Submarine melt as a potential trigger of the North East Greenland Ice Stream margin retreat during Marine Isotope Stage 3. *The Cryosphere*, *13*(7), 1911-1923.

Tabone, I., Robinson, A., Montoya, M., & Alvarez-Solas, J. (2024). Holocene thinning in central Greenland controlled by the Northeast Greenland Ice Stream. *Nature communications*, *15*(1), 6434.